ACS OMEGA

http://pubs.acs.org/journal/acsodf

Article

Multifunctional Bacterial Cellulose Films Enabled by Deep Eutectic Solvent-Extracted Lignin

Qihang Dai, Yunhua Bai, Bo Fu, and Fan Yang*

Cite This: *ACS Omega* 2023, 8, 7430−7437

Read Online

ACCESS | Metrics & More | Article Recommendations | Supporting Information

ABSTRACT: Inspired by natural plant cells, lignin is utilized as a filler and a functional agent to modify bacterial cellulose (BC). By mimicking the lignin−carbohydrate structure, deep eutectic solvent (DES)-extracted lignin serves as a glue to strength the BC films and endows the films with diverse functionality. The lignin isolated by the DES (formed by choline chloride and lactic acid) is rich in phenol hydroxyl groups (5.5 mmol/g) and exhibits a narrow molecular weight distribution. A good interface compatibility can be obtained in the composite film, and lignin fills the void/gaps between BC fibrils. The integration of lignin endows the films with enhanced water-proof, mechanical, UV shielding, gas barrier, and antioxidant abilities. The BC/lignin composite film with 0.4 g of lignin addition (BL-0.4) exhibits an oxygen permeability and a water vapor transmission rate of 0.4 mL/m^2/day/Pa and 0.9 g/m^2/day, respectively. The multifunctional films are promising candidates for packing materials and exhibit a broad application prospect in the field of petroleum-based polymer replacement.

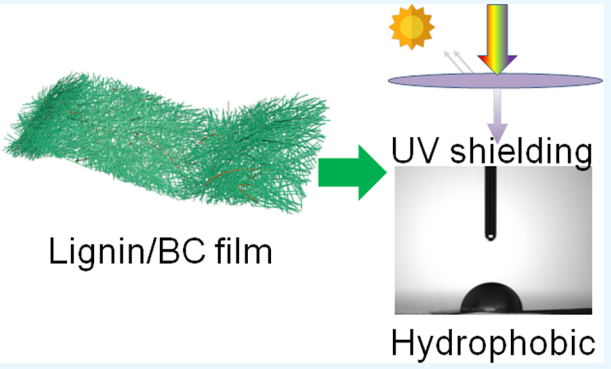

INTRODUCTION

Bacterial cellulose (BC), a masterpiece of nature, is commonly produced by *Acetobacter xylinum* or other bacteria fermentation processes.[1,2] As a biodegradable and sustainable polymer, BC possesses advantages such as superior fibril stiffness, a highly crystalline structure, and a tunable pore structure.[3] Unlike plant-derived cellulose, BC is composed of fine fibrils with ultra-high purity.[4] The abundant hydroxyl groups on BC chains make BC a potential candidate for self-standing and flexible film fabrication. However, bare BC films lack basic functionality and demonstrate limited mechanical robustness, especially under humid conditions.[5] It is urgently needed to develop BC-based films with diverse functionality and desirable mechanical performance.[6]

Fortunately, BC is viewed as a suitable substrate for hybridization because of its three-dimensional network and highly accessible hydroxyl groups.[7] Various materials have been integrated into BC films to impart the films with electronic,[8] optical,[9] hydrophobic,[10,11] and antibacterial properties.[12] To date, BC-based hybrid films have found a wide range of applications including environment remediation,[13] food packing,[14,15] energy storage,[16,17] smart sensors,[5] electromagnetic interference shielding,[18] and biomedicine.[19] Inorganic fillers such as activated carbon, zeolite, graphene oxide, metal nanoparticles, metal oxides, metal−organic frameworks, and MXenes have been used as additives for BC film modification.[20] These components are introduced into the BC skeleton by solvent evaporation-induced self-assembly, chemical crosslinking, swelling-enabled adsorption, and mechanical blending.[21,22] The incorporation of inorganic fillers might cause weak interface adhesion, leading to filler leakage and poor tolerance toward damage. Apart from inorganic fillers, petroleum-based organic chemicals including benzophenone, diisocyanate, polyvinyl alcohol, and polyethersulfone are also utilized as reinforced agents and functional ingredients to functionalize BC films.[23,24] The chemically grafting or coating of organic materials commonly involves the use of harmful and toxic reagents. Moreover, the incorporation of chemicals and inorganic fillers will deteriorate the overall biocompatibility and biodegradability of pristine BC films and has potential environmental hazards.[25]

To enhance the mechanical property and broaden the application area of BC films, the use of natural-derived polymers has gained extensive research interests.[26] Lignin, as the second abundant polymer in nature, serves as the binding agent to link adjacent cells and wraps cellulose fibrils to form a lignin−carbohydrate complex matrix in natural plants.[27] Lignin also provides water stability and mechanical rigidity for the wood cell wall,[28,29] and it can be isolated from lignocellulose *via* diverse solvents (e.g., organic solvents, organic acids, ionic

Received: September 22, 2022
Accepted: December 30, 2022
Published: February 14, 2023

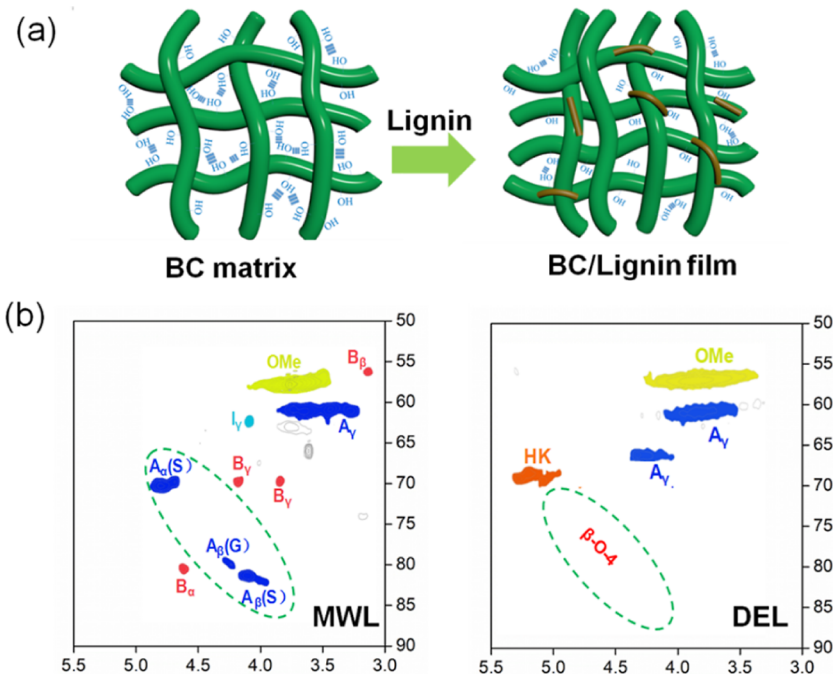

Figure 1. Schematic illustration of the film design and preparation process (a) and 2D-HSQC NMR spectra (b) of milled wood lignin (MWL) and the DEL.

liquids, and eutectic solvents) and previous studies have demonstrated that the extracted lignin exhibited excellent water-proof property, UV-blocking property, antibacterial property, and antioxidant property (AOP).[27,30,31] Incorporation of lignin into BC films to simulate the tightly linked cellulose−lignin structure is a promising strategy to prepare multifunctional films.[32] For example, Tian *et al.* fabricated BC/lignin composite films through a biosynthesis strategy.[33] There is a good affinity between lignin and BC, and the as-obtained films showed a retarded degradation property. The properties of lignin are strongly affected by its intrinsic heterogeneity, structural complexity, polydispersity in molecular weight, and structural complexity.[34]

Herein, lignin was introduced into BC to produce BC/lignin composite films *via* a facile vacuum filtration and pressing approach. In particular, the lignin was fractionated from the poplar biomass residue by using an inexpensive and recyclable deep eutectic solvent (DES) system, namely, choline chloride (ChCl) and lactic acid (LA). The ChCl−LA DES is a typical green solvent that features merits of both ionic liquids and organic solvents.[35] Highly pure, low-polarity, and phenol-rich lignin can be obtained by the DES, and a uniform dispersion of lignin in the BC film matrix can be realized. The composite films showed superior tensile strength and enhanced water resistance, UV protective, and antioxidant abilities due to the presence of lignin. Such films might open up broader prospects in the fields of food packing and electronic devices.

EXPERIMENTAL SECTION

Materials. The purified BC suspension (1 wt %) was bought from Guilin Qihong Technology Company, China. It was prepared *via* a static fermentation process with *Gluconacetobacter xylinus* strain. Choline chloride (99%, ChCl), LA (98%), and acetone were bought from Sinopharm Chemical Reagent Company. The poplar sawdust was kindly provided by Beiter Wood Industry, China.

Lignin Isolation and Composite Film Preparation. The DES solvent was prepared by mixing ChCl with LA with a molar ratio of 1:2. The mixture was heated to 80 °C under stirring to obtain a homogeneous liquid. Then, 10 g of poplar powder was added into 100 g of the DES in a round-bottom flask. After keeping it at 110 °C for 2 h, the flask was immediately put into a cold water bath to halt the reaction. The resulting liquid/solid phases were subjected to vacuum filtration, and the residues were washed with acetone (150 mL) and deionized water (150 mL). All the liquid was collected and treated in a vacuum evaporator to 30 mL. Following that, 200 mL of deionized water was added to regenerate lignin. After centrifugation, the recovered lignin was dried in a lyophilizer and kept at 4 °C for use. The details for lignin purity analysis are shown in the Supporting Information.

Under mechanical stirring, the BC suspension (100 mL) was added into a flask and stirred overnight. The DES-extracted lignin (DEL) samples of different weights (0.2, 0.4, 0.6, 0.8, and 1 g) were added into the suspension under stirring. The mixed suspension was stirred for 2 h and sonicated for another 2 h to remove air bubbles. The hydrogel films were obtained by a vacuum filtration method using polytetrafluoroethylene (pore size of 0.22 μm) as the support, and they were peeled off and fixed between two filter papers and then sandwiched between two glass plates for 48 h. The obtained films were denoted as BL-*x*, where *x* refers to the weight of lignin additives in composite films.

Characterizations. The surface and cross-section morphologies of the films were recorded by using scanning electron microscopy (SEM, JSM-7600F, Japan). All samples were clamped into holders and sputter-coated with a thin layer of Au prior to imaging tests. Atomic force microscopy (Bruker, Germany) was used to reveal the surface roughness of the films. The thermal stability of the composite films was evaluated by using thermogravimetric (TG) analysis (PerkinElmer analyzer). The temperature range was recorded from

https://doi.org/10.1021/acsomega.2c06123
ACS Omega 2023, 8, 7430−7437

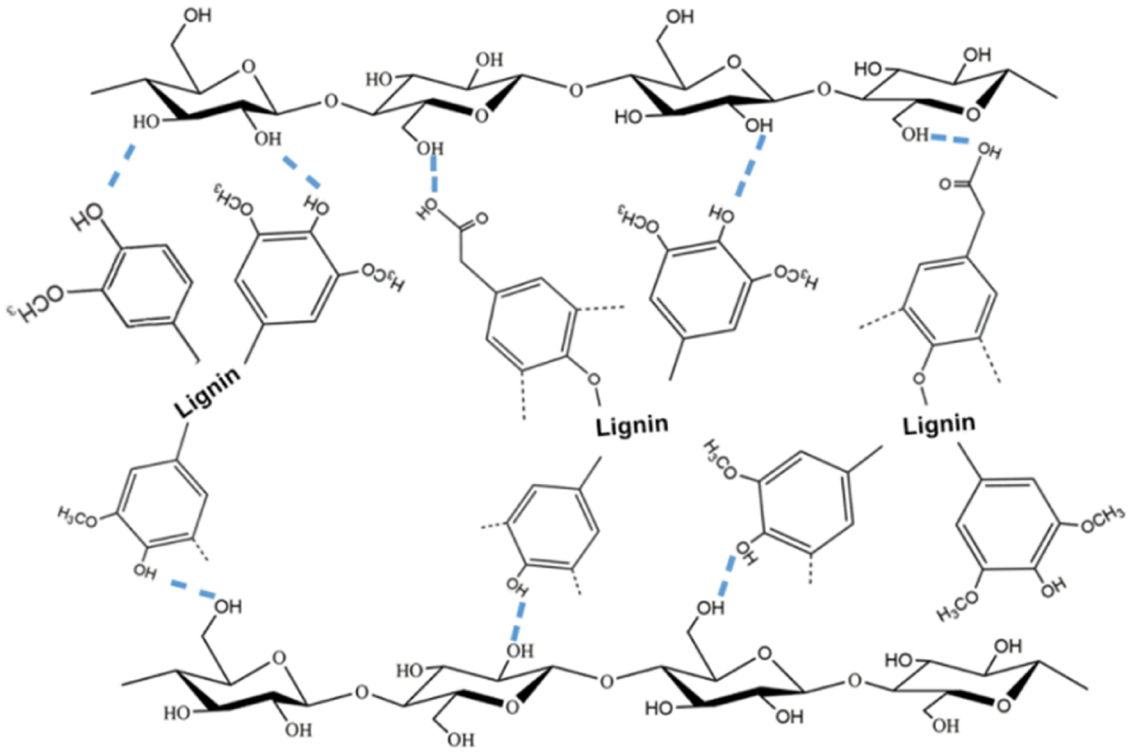

Figure 2. Schematic illustration of the crosslink between DEL and BC.

30 to 800 °C with a heating rate of 10 °C/min under N_2 protection. Fourier transform infrared (FT-IR) spectra were measured by using a Brucker Vertex-80V spectrometer over a wavenumber range of 400 to 4000 cm^{-1} at a resolution of 4 cm^{-1} to explore the lignin−cellulose interactions. The mechanical properties of films were determined using a tensile tester (Shimadzu Corporation, Japan) at a load cell of 500 N with a crosshead speed of 20 mm/min until breakage. Each sample was tested three times, and the averaged values were used. The weight-average molecular weight (M_w) and number-average molecular weight (M_n) of lignin fractions were determined by gel permeation chromatography. Approximately 4 mg of lignin was dissolved in 4.0 mL of tetrahydrofuran prior to injection. Two-dimensional heteronuclear single quantum coherence (2D-HSQC) nuclear magnetic resonance (NMR) spectra were obtained by using an AVANCE III HD 600 MHZ spectrometer for the analysis of aromatic and aliphatic chemical fractions of the lignin.

Barrier Properties. The oxygen transmission rate (cm^3/m^2/day) was estimated using a permeability tester (GDP-C, Brugger, Germany) at 25 °C and 0% relative humidity.[36] The water vapor transmission rate of the composite film was estimated using a moisture permeability tester (TSY-T1, Labthink, China) at 37 °C and 90% relative humidity. An average value was obtained from three parallel measurements.

Water Contact Angle and Water Absorption Analysis. The water contact angles were determined using a JC2000D1 Apparatus (Zhongzhen, China). Typically, 4 μL of water was dropped on the film surface, and the readings were recorded at different intervals. The water absorption ratio was analyzed by putting the films in water and recording the weight change as a function of time.

Ultraviolet Absorption and Antioxidant Tests. The ultraviolet−visible (UV−vis) transmittance of the composite films was determined using a UV-2600 spectrophotometer, and the UVA (320−400 nm) and UVB (290−320 nm) blocking properties were obtained. The AOP of the film was calculated from the free radical of 2,2′-azino-di-[3-ethylbenzothiazoline sulfonate].[36] Briefly, 1 g of the film was mixed with the radical solution (4 mL), and then, the absorbance was measured at 734 nm.

RESULTS AND DISCUSSION

Inspired by the wood cell wall, lignin−cellulose hybrid films are fabricated by dispersing DEL into BC suspension. The mixed suspension is subjected to vacuum filtration to form a wet hydrogel film. To enhance the interface compatibility between the hydrophilic cellulose and hydrophobic lignin, the wet hydrogel film is dried under an excess pressure of ca. 100 kPa. The brief illustration of the film design is demonstrated in Figure 1a. The BC matrix with a porous structure and highly available surface groups is highly accessible for lignin. The incorporation of lignin fills the spaces and voids between the interconnected cellulose fibrils, leading to a densely packed structure. The presence of excess pressure further minimizes the voids and accelerates the contact of lignin and cellulose. Similar to the natural cell wall, lignin acts as an effective binder that helps adhere and wrap adjacent cellulose fibrils. Driven by nanoscale entanglement and hydrogen bonds between lignin and cellulose fibrils, the BC/lignin composite is expected to exhibit a strong interfacial bonding, high mechanical strength, and good water stability.

In general, lignin is an irregular complex, and its structure is highly reliant on the sources and extraction processes.[37] The lignin structural characteristics have crucial effects on its multifunctional performance. To isolate lignin with a desirable property, an effective and recyclable DES composed of ChCl and LA (DES structure in Figure S1, Supporting Information) was utilized. The transparent ChCl−LA DES possesses sufficient hydrogen bonding ability and acidity, enabling the

https://doi.org/10.1021/acsomega.2c06123
ACS Omega 2023, 8, 7430−7437

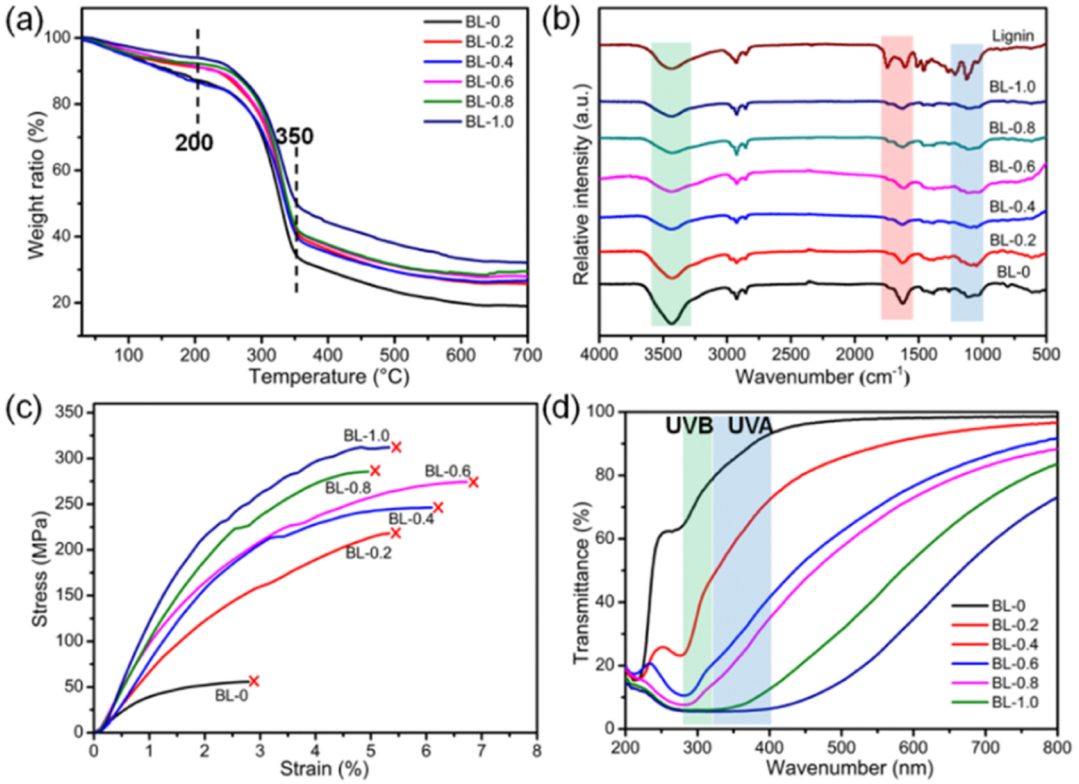

Figure 3. TG curves (a), FT-IR spectra (b), tensile properties (c), and UV−vis transmittance (d) of the BC/lignin composite films.

selective cleavage of the lignin−carbohydrate complex and realizing the dissolution of lignin.[34] Hydrophobic lignin powder is regenerated from the solution by adding water.[38] The recovered lignin shows a high purity of 93.1%, and the determined M_w and M_n are 4306 and 2393, respectively. Analyzed by the NMR technique, the chemical structural features of the DEL are summarized in Figure 1b. For comparison, milled wood lignin was used as the representative native lignin. After the DES treatment, the signals associated with β-O-4 are almost disappeared (Figure S2, Supporting Information), verifying the successful breakage of β-O-4 linkages.[39] The β-O-4 cleavage promotes the lignin dissolution and leads to the generation of Hibbert's ketone and more phenol groups.

The existence of ketone and phenol groups in the DEL would enhance the adherence of lignin on cellulose chains. The BC surface is densely functionalized with hydroxyl groups, which facilitate the adsorption/attachment of lignin molecules. In the composite film, lignin links BC fibrils together *via* hydrogen bonding (Figure 2).[40] After evaporating the water, BC/lignin composite films can be obtained from a wet hydrogel. The excess pressure endows the films with a compact structure. The film thickness determined using a micrometer is about 12 μm, and the change of the lignin ratio shows no obvious influence on the composite film thickness. When the lignin addition is over 1.0 g, lignin aggregates begin to appear in the film skeleton, and the film becomes uneven and fragile.

The physicochemical properties of the lignin-modified BC films were systematically explored. As displayed in Figure 3a, TG curves indicate that the introduction of lignin enhanced the thermal stability of composite films. There are two stages in all TG curves, which are associated with the removal of moisture (below 200 °C) and film decomposition (200−350 °C). The decomposition temperature and weight residue increase with the loadings of lignin. It can be attributed to the abundant aromatic units in DEL, which contributes to a higher thermal degradation temperature.[41] The FT-IR technique was used to identify the possible interactions between lignin and BC (Figure 3b). The recovered lignin features peaks at 1600, 1508, and 1455 cm^{-1}, corresponding to the vibrations of the lignin aromatic skeleton. In the composite BC/lignin films, these absorption signals are well-preserved and become intensified with the lignin content increase. This provides further evidence for the integration of lignin into the BC matrix.[42] The peaks centered around 3402 cm^{-1} in the pure BC film is ascribed to the −OH groups. After lignin addition, the peak intensity declines, which might be caused by the hydrogen bonding interactions between lignin and BC.[43]

The engineering stress−strain behaviors of the BC/lignin films are summarized in Figure 3c. The pure BC film (BL-0) shows a tensile strength of 47 MPa and an elongation at break of 2.9%. The incorporation of lignin enhances the mechanical property of BC films evidently. As comparison, the tensile strength and elongation at break for BL-0.2 increase to 207 MPa and 5.5%, respectively. The enhanced tensile strength is due to the lignin-induced adhesion, where lignin fills the gaps and voids between the BC fibrils. The tensile strength is positively related to the lignin ratio. By increasing the lignin addition from 0.2 to 1.0 g, the tensile strength increases gradually from 207 MPa (BL-0.2) to 343 MPa (BL-1.0). This indicates that the increased amount of lignin strengthens the hydrogen bonding network between lignin and BC. The elongation at break values of BL-0.4, BL-0.6, BL-0.8, and BL-1.0 are calculated to be 6.3, 6.9, 4.9, and 5.4%, respectively. It suggests that the presence of excess lignin would reduce the strength of interface adherence.

https://doi.org/10.1021/acsomega.2c06123
ACS Omega 2023, 8, 7430−7437

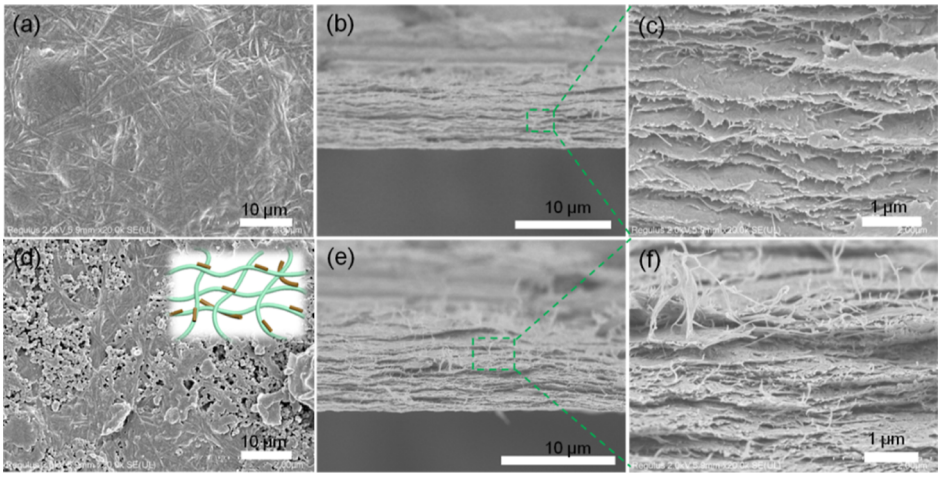

Figure 4. SEM images of the top view (a,d) and cross-section view (b,c,e,f) of BL-0 (a–c) and BL-0.4 (d–f).

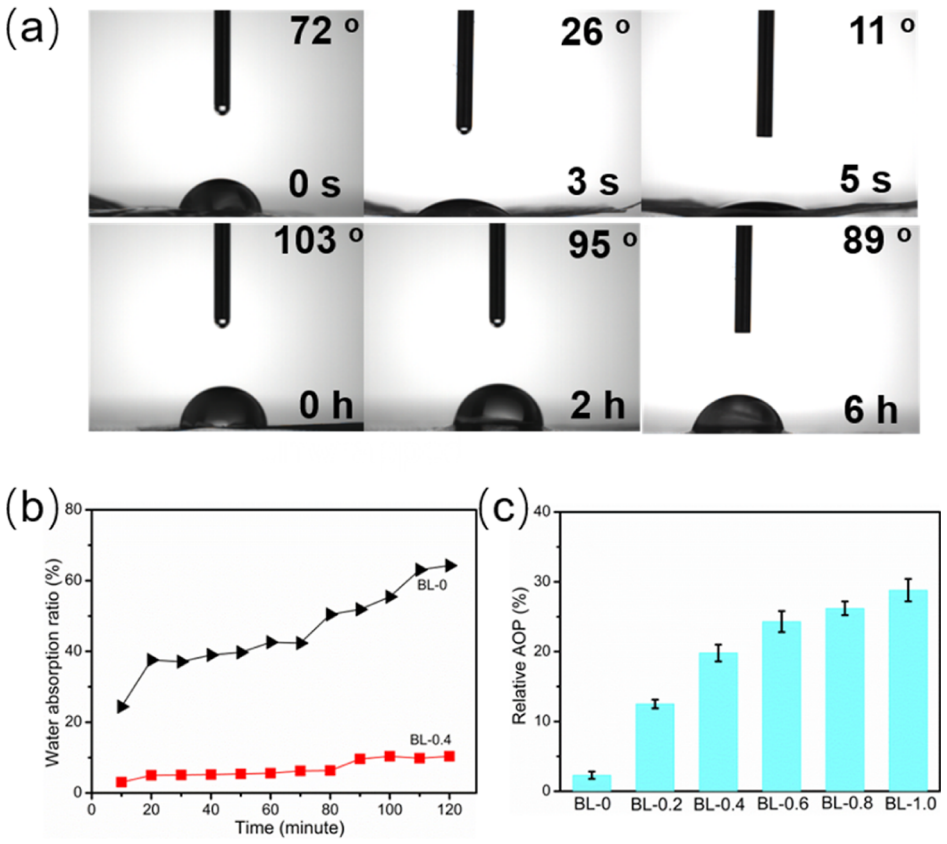

Figure 5. Water contact angles (a) and water absorption tests (b) of the BL-0 and BL-0.4 films over time and the AOP (c) of the composite films.

The optical properties of the hybrid films were explored, and all samples exhibit high transparency in the visible light range, indicating the uniform distribution of lignin in the BC matrix (Figure 3d). The introduction of lignin has adverse effects on film transparency because the chromophore groups in lignin reduce the light transmittance.[44] However, the presence of lignin imparts to the film an excellent UV blocking ability. Especially, DEL is rich in conjugated phenolic groups, ketones, and intra-molecular hydrogen bonds.[45] These groups are UV-protective and could prevent UV-induced decoloration/denaturation, rendering the composite films with potentials for packing. By increasing the lignin content to 0.8 g (BL-0.8), it could shield more than 98.6% of the UVA spectrum and 99.3% of the UVB spectrum. To prove the efficient UV-screening activity of DES-isolated lignin, commercial lignin sources such as Kraft lignin and lignosulfonate were compared. With the same lignin loading (0.4 g), DEL displays a superior UV-blocking performance (Figure S3, Supporting Information). The results verify that DEL has more UV absorption groups.[46]

In addition, the morphologies of the BL-0 and BL-0.4 films are examined to understand the effect of lignin introduction on the film structure. The neat BC film (BL-0) has a homogeneous and flat surface with a relative low surface roughness (Figures 4a and S4a, Supporting Information). BC nanofibrils are in-plane oriented and highly ordered. From the

https://doi.org/10.1021/acsomega.2c06123
ACS Omega 2023, 8, 7430−7437

cross-sectional surface, BL-0 presents a dense and laminated structure (Figure 4b). At higher resolutions, the layered structure can be clearly identified (Figure 4c). After the lignin modification, lignin occupies the voids between cellulose fibrils and adheres the BC fibrils together (Figure 4d). BC fibrils surrounded by lignin seem to be packed much denser (Figure 4e), and the surface roughness decreases from 130 to 79 nm (Figure S4b, Supporting Information). The lignin intercalation forms a more densified laminated structure and promotes the interfacial compatibility (Figure 4f).

DEL is intrinsically hydrophobic owing to its sufficient phenylpropane groups.[47] As presented in Figure 5a, the BL-0.4 film has a higher water contact angle of 103° than that of the pure BC film (72°). The water droplets quickly permeate into the hydrophilic BC film (BL-0) within 5 s. By contrast, the BL-0.4 film surface still exhibits a water contact angle of 89° after 6 h, demonstrating the superior water repellence.[48] The water absorption ability of the films was tested, and the BL-0 film has a water absorption ratio of 68%. However, the BL-0.4 film shows a very low water absorption ratio of 10%.[49] By immersing the film in water for continuous 3 days, the BL-0 film is completely disintegrated, and the shape of BL-0.4 can be maintained (Figure S5, Supporting Information). Apart from the water stability, barrier properties toward water vapor and oxygen were evaluated. BL-0 and BL-0.4 have oxygen permeability values of 0.7 and 0.4 mL/m^2/day/Pa, respectively. The higher oxygen barrier property of BL-0.4 is attributed to the presence of lignin, which repairs the film defects and creates a more complex and tortuous gas pathway. The water transmission rates of BL-0 and BL-0.4 are calculated to be 2.4 and 0.9 g/m^2/day, respectively. This is due to the hydrophobic lignin preventing the BC fibrils from water adsorption.

The composite film offers a potential solution for the sustainable and environmentally friendly food packing materials (Figure S6, Supporting Information). Also, the delayed oxidation coated by BL-0.4 is attributed to the good barrier properties against unfavorable gases of moisture and oxygen. The AOP of the films was evaluated, and the relative antioxidant power is expressed as per gram of film (Figure 5c). The active components in the films were measured by the consumed radical.[36] An increasing trend in the antioxidant activity is observed with the increase of lignin content, suggesting that the antioxidant performance is mainly originated from DEL. This is because the abundant aromatic groups in lignin could retard the radical-induced oxidation process.

CONCLUSIONS

In conclusion, based on all-natural polymers, a composite film with diverse functions and excellent mechanical performance was fabricated *via* a facile method. The lignin was isolated from poplar sawdust using an effective ChCl–LA DES system. The extracted lignin possesses a narrow molecular weight distribution and abundant phenolic hydroxyl groups. There is a good interface compatibility between lignin and BC due to the nanoscale entanglement and hydrogen bonding interactions. The composite film with the addition of 0.4 g of lignin has an oxygen permeability and a water vapor transmission rate of 0.4 mL/m^2/day/Pa and 0.9 g/m^2/day, respectively. Moreover, such composite films displayed superior mechanical strength and excellent UV resistance property and AOP. The BC/lignin films might open up broader prospects in the field of packing and electronic devices.

ASSOCIATED CONTENT

Supporting Information

The Supporting Information is available free of charge at https://pubs.acs.org/doi/10.1021/acsomega.2c06123.

Details for lignin purity analysis, formula illustration of the ChCl–LA DES, main structures observed in the extracted lignin, transparency of the composite and commercial lignin-modified films, surface roughness of lignin/BC films, water stability of lignin/BC films, and food packing potential of the composite films (PDF)

AUTHOR INFORMATION

Corresponding Author

Fan Yang − *Jiangsu Co-Innovation Center of Efficient Processing and Utilization of Forest Resources, College of Chemical Engineering, Nanjing Forestry University, Nanjing 210037, China; School of Management Science and Engineering, Nanjing University of Finance and Economics, Nanjing, Jiangsu 210023, China;* orcid.org/0000-0001-9464-0436; Email: yangfan890709@163.com

Authors

Qihang Dai − *Jiangsu Co-Innovation Center of Efficient Processing and Utilization of Forest Resources, College of Chemical Engineering, Nanjing Forestry University, Nanjing 210037, China*

Yunhua Bai − *Jiangsu Co-Innovation Center of Efficient Processing and Utilization of Forest Resources, College of Chemical Engineering, Nanjing Forestry University, Nanjing 210037, China*

Bo Fu − *Jiangsu Co-Innovation Center of Efficient Processing and Utilization of Forest Resources, College of Chemical Engineering, Nanjing Forestry University, Nanjing 210037, China;* orcid.org/0000-0002-0310-2075

Complete contact information is available at: https://pubs.acs.org/10.1021/acsomega.2c06123

Author Contributions

CRediT authorship contribution statement: Q.D.: methodology and writing—original draft. Y.B.: methodology. B.F.: conceptualization, formal analysis, investigation, and visualization. F.Y.: investigation, supervision, and project administration.

Notes

The authors declare no competing financial interest.

ACKNOWLEDGMENTS

This work was supported by the National Natural Science Foundation of China (21606133), the Jiangsu Provincial Natural Science Foundation of China (BK20160922) and the College Students' Practice and Innovation Training Project (202210298011Z). We also would like to acknowledge the support received from the Advanced Analysis & Testing Center, Nanjing Forestry University for sample tests.

REFERENCES

(1) Picheth, G. F.; Pirich, C. L.; Sierakowski, M. R.; Woehl, M. A.; Sakakibara, C. N.; de Souza, C. F.; Martin, A. A.; da Silva, R.; de

Freitas, R. A. Bacterial cellulose in biomedical applications: A review. *Int. J. Biol. Macromol.* **2017**, *104*, 97−106.
(2) Li, T.; Chen, C.; Brozena, A. H.; Zhu, J. Y.; Xu, L.; Driemeier, C.; Dai, J.; Rojas, O. J.; Isogai, A.; Wågberg, L.; Hu, L. Developing fibrillated cellulose as a sustainable technological material. *Nature* **2021**, *590*, 47−56.
(3) Cazón, P.; Vázquez, M. Bacterial cellulose as a biodegradable food packaging material: A review. *Food Hydrocolloids* **2021**, *113*, 106530.
(4) Wang, S.; Jiang, F.; Xu, X.; Kuang, Y.; Fu, K.; Hitz, E.; Hu, L. Super-Strong, Super-Stiff Macrofibers with Aligned, Long Bacterial Cellulose Nanofibers. *Adv. Mater.* **2017**, *29*, 1702498.
(5) Ma, H.; Li, X.; Lou, J.; Gu, Y.; Zhang, Y.; Jiang, Y.; Cheng, H.; Han, W. Strong bacterial cellulose-based films with natural laminar alignment for highly sensitive humidity sensors. *ACS Appl. Mater. Interfaces* **2022**, *14*, 3165−3175.
(6) Wang, J.; Chen, W.; Dong, T.; Wang, H.; Si, S.; Li, X. Enabled cellulose nanopaper with outstanding water stability and wet strength via activated residual lignin as a reinforcement. *Green Chem.* **2021**, *23*, 10062−10070.
(7) Song, L.; Shu, L.; Wang, Y.; Zhang, X.-F.; Wang, Z.; Feng, Y.; Yao, J. Metal nanoparticle-embedded bacterial cellulose aerogels via swelling-induced adsorption for nitrophenol reduction. *Int. J. Biol. Macromol.* **2020**, *143*, 922−927.
(8) Xu, T.; Du, H.; Liu, H.; Liu, W.; Zhang, X.; Si, C.; Liu, P.; Zhang, K. Advanced Nanocellulose-Based Composites for Flexible Functional Energy Storage Devices. *Adv. Mater.* **2021**, *33*, 2101368.
(9) Kaschuk, J. J.; Haj, Y. A.; Rojas, O. J.; Miettunen, K.; Abitbol, T.; Vapaavuori, J. Plant-based Structures as an Opportunity to Engineer Optical Functions in next-generation Light Management. *Adv. Mater.* **2022**, *34*, 2104473.
(10) Huang, F.; Li, Q.; Ji, G.; Tu, J.; Ding, N.; Qu, Q.; Liu, G. Oil/water separation using a lauric acid-modified, superhydrophobic cellulose composite membrane. *Mater. Chem. Phys.* **2021**, *266*, 124493.
(11) Cao, S.; Rathi, P.; Wu, X.; Ghim, D.; Jun, Y. S.; Singamaneni, S. Cellulose Nanomaterials in Interfacial Evaporators for Desalination: A "Natural" Choice. *Adv. Mater.* **2020**, *33*, 2000922.
(12) Zmejkoski, D.; Spasojević, D.; Orlovska, I.; Kozyrovska, N.; Soković, M.; Glamočlija, J.; Dmitrović, S.; Matović, B.; Tasić, N.; Maksimović, V.; Sosnin, M.; Radotić, K. Bacterial cellulose-lignin composite hydrogel as a promising agent in chronic wound healing. *Int. J. Biol. Macromol.* **2018**, *118*, 494−503.
(13) Gu, Y.; Li, H.; Ye, M.; Zhang, X.; Zhang, H.; Wang, G.; Zhang, Y. A universal route to fabricate bacterial cellulose-based composite membranes for simultaneous removal of multiple pollutants. *Chem. Commun.* **2021**, *57*, 8592−8595.
(14) Zhang, S.; Zhou, J.; Gao, X.; Zhang, H. Preparation of eco-friendly cryogel absorbent/paper mulch composite with cellulose/$ZnCl_2$ gel as adhesive. *Ind. Crops Prod.* **2022**, *177*, 114477.
(15) Nguyen, H.-L.; Tran, T. H.; Hao, L. T.; Jeon, H.; Koo, J. M.; Shin, G.; Hwang, D. S.; Hwang, S. Y.; Park, J.; Oh, D. X. Biorenewable, transparent, and oxygen/moisture barrier nanocellulose/nanochitin-based coating on polypropylene for food packaging applications. *Carbohydr. Polym.* **2021**, *271*, 118421.
(16) Asghar, M. R.; Anwar, M. T.; Xia, G.; Zhang, J. Cellulose/Poly(vinylidene fluoride hexafluoropropylene) composite membrane with titania nanoparticles for lithium-ion batteries. *Mater. Chem. Phys.* **2020**, *252*, 123122.
(17) Liu, K.; Lv, J.; Fan, G.; Wang, B.; Mao, Z.; Sui, X.; Feng, X. Flexible and robust bacterial cellulose-based ionogels with high thermoelectric properties for low-grade heat harvesting. *Adv. Funct. Mater.* **2022**, *32*, 2107105.
(18) Zhou, Z.; Song, Q.; Huang, B.; Feng, S.; Lu, C. Facile Fabrication of Densely Packed Ti_3C_2 MXene/Nanocellulose Composite Films for Enhancing Electromagnetic Interference Shielding and Electro-/Photothermal Performance. *ACS Nano* **2021**, *15*, 12405−12417.
(19) Deng, P.; Chen, F.; Zhang, H.; Chen, Y.; Zhou, J. Conductive, self-healing, adhesive, and antibacterial hydrogels based on lignin/cellulose for rapid MRSA-infected wound repairing. *ACS Appl. Mater. Interfaces* **2021**, *13*, 52333−52345.
(20) Zhang, X. F.; Wang, Z.; Ding, M.; Feng, Y.; Yao, J. Advances in cellulose-metal organic framework composites: preparation and applications. *J. Mater. Chem. A* **2021**, *9*, 23353−23363.
(21) Zhou, M.; Wang, J.; Zhao, Y.; Wang, G.; Gu, W.; Ji, G. Hierarchically porous wood-derived carbon scaffold embedded phase change materials for integrated thermal energy management, electromagnetic interference shielding and multifunctional application. *Carbon* **2021**, *183*, 515−524.
(22) Wan, Y.; Xiong, P.; Liu, J.; Feng, F.; Xun, X.; Gama, F. M.; Zhang, Q.; Yao, F.; Yang, Z.; Luo, H.; Xu, Y. Ultrathin, strong, and highly flexible $Ti_3C_2T_x$ MXene/bacterial cellulose composite films for high-performance electromagnetic interference shielding. *ACS Nano* **2021**, *15*, 8439−8449.
(23) Zhang, X.; Liu, W.; Sun, D.; Huang, J.; Qiu, X.; Li, Z.; Wu, X. Very Strong, Super-Tough, Antibacterial, and Biodegradable Polymeric Materials with Excellent UV-Blocking Performance. *Chemsuschem* **2020**, *13*, 4974−4984.
(24) Cheng, Q.; Li, Q.; Yuan, Z.; Li, S.; Xin, J. H.; Ye, D. Bifunctional Regenerated Cellulose/Polyaniline/Nanosilver Fibers as a Catalyst/Bactericide for Water Decontamination. *ACS Appl. Mater. Interfaces* **2021**, *13*, 4410−4418.
(25) da Costa Lopes, A. M.; Gomes, J. R. B.; Coutinho, J. A. P.; Silvestre, A. J. D. Novel insights into biomass delignification with acidic deep eutectic solvents: a mechanistic study of β-O-4 ether bond cleavage and the role of the halide counterion in the catalytic performance. *Green Chem.* **2020**, *22*, 2474−2487.
(26) Liu, C.; Li, M.-C.; Chen, W.; Huang, R.; Hong, S.; Wu, Q.; Mei, C. Production of lignin-containing cellulose nanofibers using deep eutectic solvents for UV-absorbing polymer reinforcement. *Carbohydr. Polym.* **2020**, *246*, 116548.
(27) Ragauskas, A. J.; Beckham, G. T.; Biddy, M. J.; Chandra, R.; Chen, F.; Davis, M. F.; Davison, B. H.; Dixon, R. A.; Gilna, P.; Keller, M.; Langan, P.; Naskar, A. K.; Saddler, J. N.; Tschaplinski, T. J.; Tuskan, G. A.; Wyman, C. E. Lignin Valorization: Improving Lignin Processing in the Biorefinery. *Science* **2014**, *344*, 1246843.
(28) Song, Y.; Chen, S.; Chen, Y.; Xu, Y.; Xu, F. Biodegradable and transparent films with tunable UV-blocking property from Lignocellulosic waste by a top-down approach. *Cellulose* **2021**, *28*, 8629−8640.
(29) Cusola, O.; Rojas, O. J.; Roncero, M. B. Lignin Particles for Multifunctional Membranes, Antioxidative Microfiltration, Patterning, and 3D Structuring. *ACS Appl. Mater. Interfaces* **2019**, *11*, 45226−45236.
(30) Guo, D.; Guo, Y.; Sha, L.; Lyu, G.; Li, J.; Zhang, X.; Liu, B. Subcritical Ethanol Catalyzed with Deep Eutectic Solvent Extract Phenolic Lignin for Preparation of an Ultraviolet-Blocking Composite Film. *Energy Fuels* **2020**, *34*, 8395−8402.
(31) Shojaeiarani, J.; Bajwa, D. S.; Ryan, C.; Kane, S. Enhancing UV-shielding and mechanical properties of polylactic acid nanocomposites by adding lignin coated cellulose nanocrystals. *Ind. Crops Prod.* **2022**, *183*, 114904.
(32) Upton, B. M.; Kasko, A. M. Strategies for the conversion of lignin to high-value polymeric materials: review and perspective. *Chem. Rev.* **2015**, *116*, 2275−2306.
(33) Tian, D.; Guo, Y.; Huang, M.; Zhao, L.; Deng, S.; Deng, O.; Zhou, W.; Hu, J.; Shen, F. Bacterial cellulose/lignin nanoparticles composite films with retarded biodegradability. *Carbohydr. Polym.* **2021**, *274*, 118656.
(34) Hong, S.; Shen, X. J.; Xue, Z. M.; Sun, Z. H.; Yuan, T. Q. Structure-function relationships of deep eutectic solvents for lignin extraction and chemical transformation. *Green Chem.* **2020**, *22*, 7219−7232.
(35) Su, Y.; Huang, C.; Lai, C.; Yong, Q. Green solvent pretreatment for enhanced production of sugars and antioxidative lignin from poplar. *Bioresour. Technol.* **2021**, *321*, 124471.

https://doi.org/10.1021/acsomega.2c06123
ACS Omega 2023, 8, 7430−7437

(36) Espinosa, E.; Bascón-Villegas, I.; Rosal, A.; Pérez-Rodríguez, F.; Chinga-Carrasco, G.; Rodríguez, A. PVA/(ligno)nanocellulose biocomposite films. Effect of residual lignin content on structural, mechanical, barrier and antioxidant properties. *Int. J. Biol. Macromol.* **2019**, *141*, 197−206.
(37) Hong, S.; Shen, X. J.; Pang, B.; Xue, Z. M.; Cao, X.-F.; Wen, J.-L.; Sun, Z.-H.; Lam, S. S.; Yuan, T.-Q.; Sun, R.-C. In-depth interpretation of the structural changes of lignin and formation of diketones during acidic deep eutectic solvent pretreatment. *Green Chem.* **2020**, *22*, 1851−1858.
(38) Zhang, X.-F.; Wang, Z.; Song, L.; Feng, Y.; Yao, J. Chinese ink enabled wood evaporator for continuous water desalination. *Desalination* **2020**, *496*, 114727.
(39) Xia, Q.; Chen, C.; Yao, Y.; Li, J.; He, S.; Zhou, Y.; Li, T.; Pan, X.; Yao, Y.; Hu, L. A strong, biodegradable and recyclable lignocellulosic bioplastic. *Nat. Sustain.* **2021**, *4*, 627.
(40) Jiang, J.; Carrillo-Enríquez, N. C.; Oguzlu, H.; Han, X.; Bi, R.; Saddler, J. N.; Sun, R. C.; Jiang, F. Acidic deep eutectic solvent assisted isolation of lignin containing nanocellulose from thermo-mechanical pulp. *Carbohydr. Polym.* **2020**, *247*, 116727.
(41) Wei, Z.; Cai, C.; Huang, Y.; Wang, P.; Song, J.; Deng, L.; Fu, Y. Strong biodegradable cellulose materials with improved crystallinity via hydrogen bonding tailoring strategy for UV blocking and antioxidant activity. *Int. J. Biol. Macromol.* **2020**, *164*, 27−36.
(42) Bian, H.; Chen, L.; Dong, M.; Wang, L.; Wang, R.; Zhou, X.; Wu, C.; Wang, X.; Ji, X.; Dai, H. Natural lignocellulosic nanofibril film with excellent ultraviolet blocking performance and robust environment resistance. *Int. J. Biol. Macromol.* **2021**, *166*, 1578−1585.
(43) Sadeghifar, H.; Venditti, R.; Jur, J.; Gorga, R. E.; Pawlak, J. J. Cellulose-Lignin Biodegradable and Flexible UV Protection Film. *ACS Sustainable Chem. Eng.* **2017**, *5*, 625−631.
(44) Zhang, X. F.; Song, L.; Wang, Z.; Wang, Y.; Wan, L.; Yao, J. Highly transparent graphene oxide/cellulose composite film bearing ultraviolet shielding property. *Int. J. Biol. Macromol.* **2020**, *145*, 663−667.
(45) Tran, M. H.; Phan, D.-P.; Lee, E. Y. Review on lignin modifications toward natural UV protection ingredient for lignin-based sunscreens. *Green Chem.* **2021**, *23*, 4633−4646.
(46) Wang, Z. K.; Hong, S.; Wen, J. L.; Ma, C. Y.; Tang, L.; Jiang, H.; Chen, J. J.; Li, S.; Shen, X. J.; Yuan, T. Q. Lewis acid-facilitated deep eutectic solvent (DES) pretreatment for producing high-purity and antioxidative lignin. *ACS Sustainable Chem. Eng.* **2020**, *8*, 1050−1057.
(47) Borrega, M.; Päärnilä, S.; Greca, L. G.; Jääskeläinen, A.-S.; Ohra-aho, T.; Rojas, O. J.; Tamminen, T. Morphological and wettability properties of thin coating films produced from technical lignins. *Langmuir* **2020**, *36*, 9675−9684.
(48) Zhang, X.-F.; Song, L.; Chen, X.; Wang, Y.; Feng, Y.; Yao, J. Zirconium ion modified melamine sponge for oil and organic solvent cleanup. *J. Colloid Interface Sci.* **2020**, *566*, 242−247.
(49) Zhang, X.-F.; Wang, Z.; Song, L.; Yao, J. In situ growth of ZIF-8 within wood channels for water pollutants removal. *Sep. Purif. Technol.* **2021**, *266*, 118527.

https://doi.org/10.1021/acsomega.2c06123
ACS Omega 2023, 8, 7430−7437